# Evaluating the Calibration and Validation of the Clouds and the Earth's Radiant Energy System (CERES) instruments on Terra and Aqua over twenty years

Mohan Shankar, Norman Loeb, Nathaniel Smith, Natividad Smith, Janet Daniels, Susan Thomas, and Dale Walikainen

***Abstract*— Six Clouds and the Earth's Radiant Energy System (CERES) instruments on four satellites are used to produce a global continuous multi-decadal record of Earth's radiation budget (ERB) at the top-of-atmosphere (TOA). Each CERES instrument was calibrated and characterized on the ground before launch, while post-launch calibration is conducted using on-board calibration sources. The performance of the CERES instruments is verified using vicarious approaches involving both Earth and celestial targets. In this paper, we describe the calibration and validation approach and demonstrate the performance of the CERES instruments on the Terra and Aqua spacecrafts over the twenty-year period since launch. Validation results demonstrate that after applying the appropriate calibration corrections, all four instruments are stable and perform consistently with each other. Comparisons of observations between instruments on the two spacecrafts during orbital crossings further confirm the consistent performance across all instruments over the twenty-year period.**

***Index Terms*—Terra, Aqua, CERES, calibration, radiometry, validation.**

## I. INTRODUCTION

THE Clouds and the Earth's Radiant Energy System (CERES) project combines measurements from CERES instruments and several other data sources to produce a global continuous record of the Earth's radiation budget (ERB) at the top-of-atmosphere (TOA), within the atmosphere and surface for a range of time and spatial scales [1,2]. Six CERES instruments measuring broadband reflected solar and emitted thermal infrared radiation from Earth are currently flying on four spacecraft: Flight Models (FMs) 1 and 2 on Terra launched in December 1999; FMs 3 and 4 on Aqua launched in May 2002; FM5 on Suomi National Polar-orbiting Partnership (SNPP) launched in October 2011; and FM6 on NOAA-20 launched in November 2017. All spacecraft were launched into a polar sun-synchronous orbit with Terra and Aqua at an altitude of 705km, and SNPP and NOAA-20 spacecraft at an altitude of 824km. Terra has a 1030 mean local time (MLT) equatorial crossing time, while Aqua, SNPP and NOAA20 have a 1330 MLT equatorial crossing time. All CERES instruments are operating well past their design lifetime of 5 years. Starting in 2022, the Terra and Aqua orbits began to drift to earlier and later MLTs, respectively. Should the missions remain healthy and be allowed to continue, Terra and Aqua will cross 0900 and 1500 MLTs in 2026, marking the last year of science operations.

The pre-launch accuracy goals for the CERES instruments are 0.5% in the emitted thermal bands and 1% in the reflected solar bands, defined at 1-sigma confidence intervals (CI). These accuracy goals are achieved by an extensive pre-launch calibration and characterization program and tracked in-flight using on-orbit calibration sources. Vicarious validation studies are performed using various Earth targets as well as the Moon to evaluate instrument performance.

In this paper, we demonstrate the long-term performance of the four CERES instruments on Terra and Aqua during twenty years of continuous operations, after the application of the most up-to-date corrections for instrument drift identified by the on-board calibration sources in conjunction with the various validation studies using vicarious targets. These updates are incorporated in the publicly available Edition 4 data products for Terra and Aqua. We also show intercomparisons between the instruments across the two spacecraft.

## II. BACKGROUND

### *A. CERES Instrument*

The CERES instruments were designed, developed, and calibrated by Northrop Grumman Aerospace Systems (NGAS, formerly TRW) before being integrated onto each spacecraft.

Mohan Shankar is with NASA Langley Research Center, Hampton, VA 23666 USA (e-mail: mohan.shankar-1@nasa.gov).

Norman Loeb is with NASA Langley Research Center, Hampton, VA 23666 USA (e-mail: norman.g.loeb@nasa.gov).

Nathaniel Smith is with ADNET Systems, USA (e-mail: nathaniel.p.smith@nasa.gov).

Natividad Smith is with Analytical Mechanics Associates Inc., Hampton, VA 23666 USA (e-mail: nitchie.smith@nasa.gov).

Janet Daniels is with Analytical Mechanics Inc., Hampton, VA 23666 USA (e-mail: janet.l.daniels@nasa.gov).

Susan Thomas is with Science Systems and Applications Inc., Hampton, VA 23666 USA (e-mail: susan.thomas-1@nasa.gov).

Dale Walikainen is with ADNET Systems, USA (e-mail: dale.r.walikainen@nasa.gov).

Color versions of one or more of the figures in this article are available online at http://ieeexplore.ieee.org

Each CERES instrument carries three sensor assemblies, each with identical Cassegrain f/1.8 telescopes and thermistor bolometer detectors. The sensor assemblies correspond to the three spectral channels - a Shortwave (SW) channel that measures the Earth reflected radiances in the 0.3-5$\mu$m spectral range, a Total channel (TOT) that measures the total radiance leaving the Earth, spanning the spectral range of 0.3-200$\mu$m, and a Window channel (WN) that measures the Earth emitted thermal radiances in the spectral range of 8-12$\mu$m (for the instruments on Terra, Aqua and SNPP). The CERES instrument on NOAA-20 carries a longwave (LW) channel that spans the 5-35$\mu$m spectral range, which replaces the WN channel on all prior instruments. Fig. 1 is a drawing of the CERES instrument, showing the various components. The sensor assemblies are coaligned and mounted on a single scan head such that the fields of view of the three channels overlap each other by approximately 98%. The scan head can be rotated about its elevation axis as it scans the Earth every 6.6s. It can also be commanded to rotate about the azimuth axis, for increased angular sampling or for conducting special measurement campaigns. The instruments also carry onboard calibration sources (within the instrument structure) to detect and track any changes to channel performance. The MAM baffles are the port through which Sun illuminates the solar diffuser used for solar calibration.

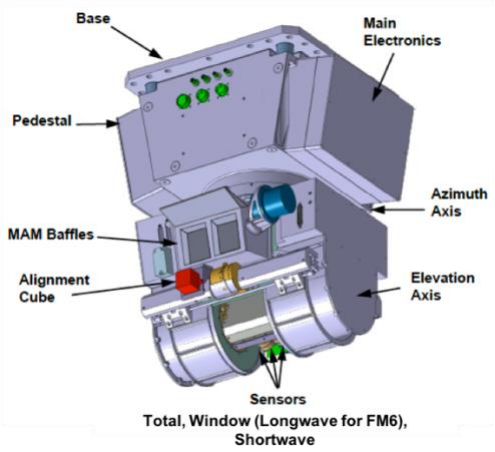


**Fig. 1.** Drawing of the CERES instrument showing the various components.

A cross-section of one of the three sensor assemblies on the CERES instrument is shown in Fig. 2. Each assembly consists of a forward baffle, telescope, and detector. The forward baffle restricts the Field of View (FOV) and blocks out stray energy from entering the telescope. The telescope optical system consists of primary and secondary mirrors of the Cassegrain telescope and the optical filters. The FOV of the telescope is a truncated diamond shape that is 1.3 degrees wide and 2.6 degrees tall, as defined by the field stop placed behind the primary mirror. A pair of filters are used for each of the SW and WN channels, with one located on the spider holding the secondary mirror, while the second filter located in between the field stop and the bolometer detector. The TOT channel does not have filters and therefore measures all the energy that arrives at the telescope.

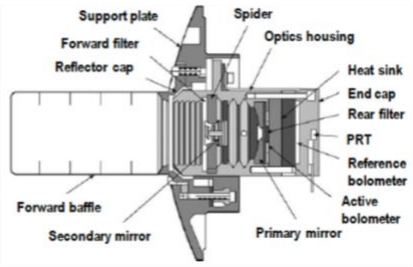


**Fig. 2.** The cross-section of a CERES sensor assembly showing the optical components and the detector. The Forward and Rear filters are for the SW and WN sensor. The TOT sensor does not have any filters in its optical path.

The thermistor bolometer detector consists of an active and a reference bolometer flake which are mounted on separate assemblies that are in thermal contact with each other and with a heatsink maintained at a constant temperature of 38 $^0$C using an electrical heater. Both the active and reference bolometers are covered with layers of Aeroglaze-Z-306 doped with 10% carbon black which serve as absorbers.

*B. On-board Calibration Systems*

To detect any drifts in the responses of the channels, each CERES instrument is equipped with two in-flight calibration systems- the Internal Calibration Module (ICM) and the Mirror Attenuator Mosaic (MAM). The ICM consists of two blackbody sources for calibrating the TOT and WN channels as well as a shortwave internal calibration source (SWICS) for calibrating the SW channel. The blackbodies are 2.75cm in diameter, concentric grooved and made of anodized black aluminum. Platinum Resistance Thermometers (PRT) are embedded in the blackbodies to measure the temperature of the blackbodies' emitting surface. The SWICS consists of an evacuated tungsten halogen lamp, a diffuser, and a fold mirror to direct the light to the CERES SW telescope. A silicon photodetector is used to measure the light that is reflected by the fold mirror to the SW telescope.

The MAM is a solar diffuser plate that is used for calibration of the SW and TOT channels. The MAM consists of a baffle and a solar diffuser plate which attenuates and diffuses solar radiation that the SW and TOT channels can view. The solar diffuser plate consists of an array of spherical aluminum mirror segments that are separated by an absorbing black paint surface. The MAMs on Terra and Aqua demonstrated anomalous on-orbit behavior and therefore were not used for instrument calibration [3].

*C. Operational Modes*

The CERES instrument has two gimbals that provide the capability of scanning in both the elevation and azimuth axes independently. The primary mode of operation is the Fixed Azimuth Plane Scan (FAPS) mode or Cross-track mode, where the azimuth gimbal is kept fixed and the sensor assembly rotates only about the elevation axis, perpendicular to the orbital path.

During each scan, the sensor assembly scans back and forth about its elevation axis. The scan starts with a view of space on one side of Earth, view of Earth from one limb to the other, view of space on the other side of Earth and further within the instrument structure to view the ICM before retracing. CERES instruments have spent most of their operational time in the FAPS mode, providing daily global coverage of Earth. The secondary mode of operation is the Rotating Azimuth Plane Scan (RAPS), where the azimuth and elevation gimbals are active simultaneously. This scan mode provides increased angular sampling of the Earth and is therefore used for data collects to support the development of Angular Distribution Models (ADM) to convert the instrument observed directional radiances into total hemispherical fluxes at the TOA [4]. The Programmable Azimuth Plane Scan (PAPS) scan mode is a modification of the RAPS mode which aims to increase the sampling over a specific Earth target as the spacecraft flies by it. In this mode, the instrument head is rotated so that the Earth target lies in the scan plane, or the scan plane orientation follows a prescribed schedule. The relative azimuth of the scan head is adjusted as the satellite moves along its orbit, based on the desired application.

The scanning modes of the two instruments on Terra and Aqua were alternated between the FAPS and RAPS modes every three months for the first two years in the mission following which the modes were fixed, with one instrument on each spacecraft placed in the FAPS mode (FM1, FM4) and the others in RAPS mode. The four instruments on Terra and Aqua were to be placed in the FAPS mode in June 2005. However, in April 2005, the SW sensor on FM4 malfunctioned and thus, both FM3 and FM4 instruments were placed in the FAPS mode in April 2005.

As part of eventual decommissioning of the Terra and Aqua spacecraft, the orbits of Terra and Aqua have been allowed to drift from their nominal equatorial MLT crossings, with Terra starting in April 2021, while Aqua starting in January 2022. The CERES team is using this opportunity to collect measurements to serve various scientific needs. In 2021, the FM2 (November) and FM4 (July) instruments were placed into RAPS mode to collect angular data as the MLT drifts, to help validate the ADMs.

### *D. Measurement Equation*

The radiance that arrives at the CERES telescope, called unfiltered radiance, is focused (and filtered) by the telescope optics onto the detector. The radiance arriving at the detector, called filtered radiance, results in an analog voltage signal that is sampled and processed by the detector electronics to convert them to digital counts. Radiometric count conversion algorithms convert the digital counts into filtered radiances using radiometric gains. These radiometric gains are derived during instrument pre-launch calibrations and changes to the gains are monitored in-flight using the onboard calibration sources.

The filtered radiance for any CERES channel is the product of the scene spectral radiance and the spectral response function (SRF) of the CERES channel, integrated over all wavelengths. The SRF of the channel is the combined transmission of all surfaces in the optical path, which includes the optical filters (SW and WN channels), the reflectance of the primary and secondary mirrors and the black absorbance of the detector. The filtered radiance is specified as the product of the channel digital counts with the radiometric gain of the sensor channel. Mathematically, the general equation that expresses this measurement for any channel is given by:

$$I_f = \int_{\lambda=0}^{\infty} S_\lambda I_\lambda d\lambda = A_v * Counts, \quad (1)$$

where $I_f$ represents the filtered radiance, $S_\lambda$ represents the sensor channel's spectral response function, and $I_\lambda$ is the spectral radiance of the target being viewed. $A_v$ represents the broadband radiometric gain of the channel. The radiometric gain and the SRFs of all instruments are characterized on the ground pre-launch [5,6]. The radiometric gain is monitored post-launch using the on-board ICM.

For science applications, there is a need to obtain the unfiltered radiances at the Earth's TOA, which removes the influence of the instrument SRF. In addition, the Earth's TOA radiance needs to be unambiguously split into two spectral bins: Earth reflected solar and Earth emitted thermal energy. The unfiltered radiances are obtained from the measured filtered radiances using an unfiltering algorithm, which utilizes the channel's SRF and a database of simulated spectra of Earth scenes under various atmospheric and viewing conditions to obtain a set of coefficients used for this conversion [7].

### *E. Pre-Launch Calibration and Characterization*

To ensure that the CERES instrument meets the measurement accuracy goals, it is first put through an extensive pre-launch calibration campaign. The calibration campaign establishes the instruments' absolute accuracy traceable to a known reference standard. After determining and applying pre-launch to post-launch calibration adjustments, any instrument drifts are identified and accounted for by using the ICM.

The absolute calibration for the CERES instruments was performed by NGAS using a custom-built Radiometric Calibration Facility (RCF) to fully evaluate the performance of the instrument in the expected operational environment [5]. The absolute calibration for the TOT and WN channels was performed using a blackbody source tied to the International Temperature Scale of 1990. The blackbody source along with a Transfer Active Cavity Radiometer (TACR) was used to calibrate the Shortwave Reference Source (SWRS), which in turn was used to bring the SW channel to the same calibration reference. The radiometric gains for all channels were also determined using the ICM during the pre-launch calibrations. In addition, several other characterizations were conducted which included point response measurements as well measurements of each channel's SRFs, all of which are used in the generation of the higher-level data products.

### *F. Data Products*

The data products used for all the results shown in this paper are the Edition 4 data products, which are the most up-to-date versions currently available for public distribution. These

products incorporate all updates to instrument coefficients and algorithms over previous versions of the data products. The data products for the instruments are shown in the table below along with the analysis used for the correction. In addition to the time varying gains and SRFs, the CERES instruments are set to a common radiometric scale of FM1 on Terra through a single radiometric adjustment at the start of mission [8]. A description of the various data product levels is provided on the CERES website (https://ceres.larc.nasa.gov/data/documentation).

| Spacecraft/instrument | Version | Gains | Spectral Response Functions (SRF) | Analysis used for SRF Correction |
|---|---|---|---|---|
| *Terra/FM1, FM2 Aqua/FM3, FM4* | *Edition 4* | *Time Varying* | *Time-varying SRF changes in SW for the instrument operating in RAPS mode.* | *Nadir direct comparison of clear ocean scenes* |
| | | | *Time-varying SRF changes in the SW portion of TOT.* | *Regression of day-night differences between LW and WN tropical all-sky ocean and all-sky land radiances.* |

**Table 1.** Version of data products used for the analysis in this paper.

## III. Post-Launch Instrument Corrections

After launch, the primary means of identifying and correcting for changes in the broadband response of all CERES channels is by using the ICM. The use of the ICM during pre-launch calibrations provides traceability of the post-launch calibrations to known ground references. In addition to the broadband gain, the SRFs of the SW and TOT channels were determined to need corrections. In this section, we provide an overview of the on-orbit calibration process to account for changes in the broadband gain. We also briefly discuss the SRF changes that have been applied to the SW and TOT channels.

### *A. Instrument Gain*

The changes in gains of the CERES channels are monitored by periodic calibrations with the onboard ICM. The calibration of the three channels using the ICM are performed three times weekly. Although the ICM is viewed by the telescopes during every Earth scan, it is only active during actual calibration sequences. Calibrations for the TOT and WN channels involve views of the blackbodies set to temperatures of 295K, 305K and 315K. The gain for the TOT and WN channels is calculated by performing a linear regression between the digital counts from the channel and the calculated radiance from the blackbody over the range of temperatures it is operated over. The calibration of the SW channel is performed by views of the SWICS operated at three predetermined levels equivalent to brightness temperatures of 2100K (Level-3), 1900K (Level-2) and 1700K (Level-1). The time-varying change in gain for the SW channel is tracked by monitoring the channel response to the SWICS operated at Level-2.

For each instrument, the gain for any channel is computed monthly by averaging all the calibrations conducted in the month. The observed changes in the gain are used in the calculation of the filtered radiances from the digital counts for each CERES footprint using Eq.1. The Terra and Aqua Edition 4 data products utilize the most up-to-date algorithms and coefficients released by the CERES team (Table 1). For the CERES instruments on Terra and Aqua, the Edition 4 gain for a given month is computed using a 5-month running mean of the monthly average gain value for the TOT and WN channels, centered on the given month, as input for processing. The 5-month running mean was replaced with a 3-month running mean, beginning in July 2020 to reduce the latency of the data products. For the SW channels, a monthly average gain value is used.

Changes in CERES instrument gains for the three channels on Terra and Aqua as tracked by the ICM are shown in Fig. 3 and Fig. 4, respectively. These gain changes are accounted for in all CERES Edition 4 data products.


**Fig. 3.** Percent change in gain for all channels from March 2000- July 2022, normalized to the start of the mission for CERES Terra (a) FM1 and (b) FM2.

Relative to March 2000, the FM1 instrument gain for the TOT channel response increased by ≈0.75%, the SW channel response decreased by ≈0.1%, and the WN channel response initially decreased before rising to ≈0.5% (Fig. 3(a)). For FM2, the TOT channel response increased by ≈0.9%, the SW channel response decreased by ≈0.6%, and the WN channel response showed a net 0.1% increase following an initial drop (Fig. 3(b)).

On Aqua, the FM3 TOT channel's response increased by ≈0.8%, the SW channel response increased by ≈0.4% while the WN channel response decreased by ≈0.8% since the start of the Aqua mission (Fig. 4(a)). For the FM4 instrument, the TOT channel response increased by ≈1.2%, the SW channel response increased by ≈0.6% through March 2005 at which point it failed (Fig. 4(b)). The WN channel showed a response increase of ≈0.25% since July 2002.

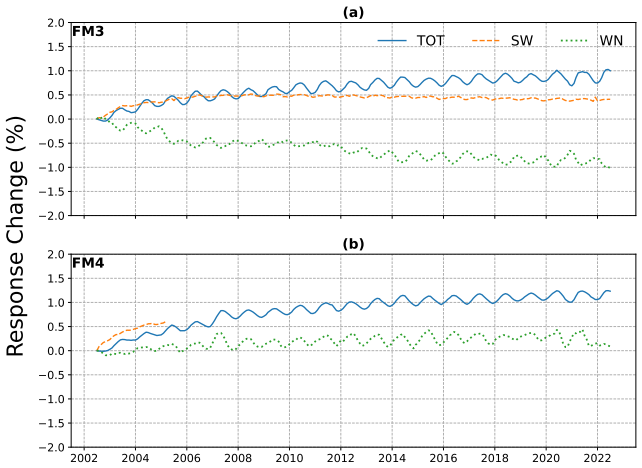


**Fig. 4.** Percent change in gain for all channels from July 2002- July 2022, normalized to the start of the mission for CERES Aqua (a) FM3 and (b) FM4.

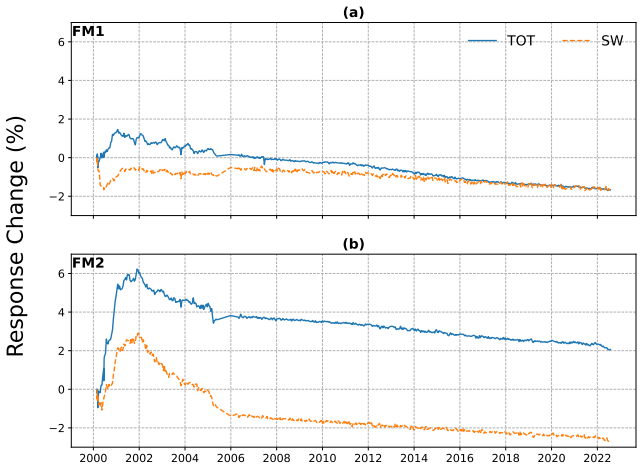


**Fig. 5.** Percent change in response of the TOT and SW channels during solar calibrations from March 2000- July 2022, normalized to the start of mission CERES Terra (a) FM1 and (b) FM2.

*B. Solar Calibration*

Each CERES instrument carries a MAM which diffuses and attenuates sunlight for the SW and TOT channels to view. The MAM provides a broadband source that spans the spectral range of the SW channel as well as the SW portion of the TOT channel. The solar observation protocol initially used a 'Classical' approach which involved rotating the instrument in the azimuth axis to point the MAM towards the sun while the sensors would scan in the elevation axis to alternate between viewing the MAM and deep space. The protocol was switched to using a 'Raster' approach in 2006 (January 2006 for Terra and February 2006 for the Aqua instruments) to reduce the duration of solar exposure of the MAM during each calibration event, thereby reducing optical degradation of the MAM. This involves parking the telescopes viewing the MAM before the start of the calibration. The instrument then rotates in Azimuth to emulate a raster scan, viewing space on either side of the MAM as the Sun drifts down the MAM for the duration of the calibration event.

Solar calibrations are conducted twice a month. The process of reducing the data from a solar calibration event for the two scenarios defined above is described by Wilson et al. [9]. Figs. 5 and 6 show the response of the SW and TOT channels of the instruments on Terra and Aqua while viewing the MAM. The plots show the percent change of the channel digital counts normalized to the first month of the mission. It is important to note that no gain or SRF adjustments have been incorporated into the analysis presented here.

For all four instruments, the SW and TOT channel responses showed a large variation (as large as 6% for FM2 TOT channel) during the first few years since the start of their missions. This is attributed to changes in the MAM surface with a most likely cause being fabrication anomalies and subsequent oxidation of the MAM surfaces post launch [10]. The first few years of the missions also corresponds to a period during which the instruments were cycled between the RAPS and FAPS mode of operations, which resulted in a wavelength dependent optical degradation of the telescopes [11].

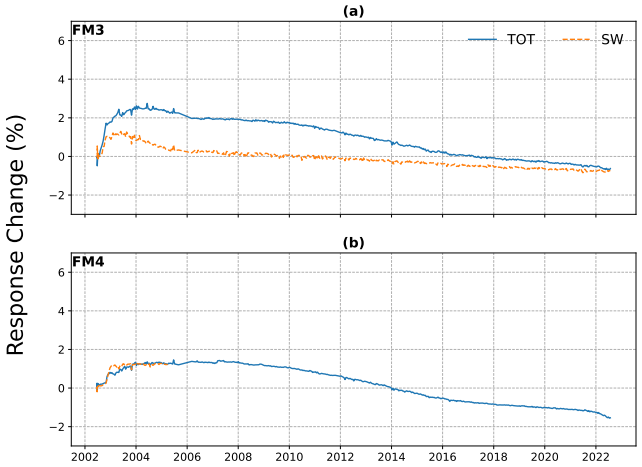


**Fig. 6.** Percent change in response of the TOT and SW channels during solar calibrations from July 2002- July 2022, normalized to the start of mission CERES Aqua (a) FM3 and (b) FM4.

It is seen in Figs. 5 and 6 that the variability of the solar calibration response reduced significantly after transitioning to the 'Raster' approach. Owing to the large variations observed in the early years, the solar observations were not used for calibrating the CERES instruments. Nonetheless, the data are useful to help identify any anomalous or long-term change in instrument behavior. For example, the slight change in response due to a switch in instrument operational mode from crosstrack

to RAPS for FM2 in November 2021 (Fig. 5(b)) and FM4 in July 2021 (Fig. 6(b)) is detectible. The longer-term drop in the response after March 2005 is attributed to the slow degradation of the MAM surface, which for the SW channels on FMs 1, 2 and 3 is between 2-2.5% through July 2022, while for the TOT channels, it is between 1.5-2%.

### *C. Post-Launch Spectral Response Adjustments*

The CERES on-board calibration sources do not cover the entire spectral range of CERES measurements. Various vicarious validation methods are typically used to evaluate the CERES instrument performance over various spatial, temporal, and spectral scales. Early analysis of CERES SW validation data indicated that decreases in albedo for clear ocean scenes were far more pronounced than those for cloudy scenes or other scene types. In addition, a direct comparison of coincident CERES nadir radiances from instrument pairs on Terra and Aqua depended on the instrument scan mode with larger degradation being associated with the instrument operating in the RAPS mode [11]. The wavelength dependent degradation in the SW channel is represented by [12,13]:

$$T(\lambda) = 1 - e^{-\alpha\lambda}, \quad (2)$$

where $\alpha$ is the coefficient of the fit to the data, and λ is the wavelength. Each month, a unique parameter $\alpha$ is derived for the instrument on Terra and Aqua that is operating in the RAPS mode through a direct comparison of observations between the two instruments on a single spacecraft. We assume that SW spectral degradation only occurs when an instrument is operated in RAPS mode.

The unfiltered emitted thermal radiance at night is determined directly from the filtered TOT channel measurements while those for the day are obtained from the TOT and SW channels [7]. Analysis of long-term trends of global day minus night LW anomalies demonstrated a need for an adjustment to the SW portion of the TOT channel SRF on the instruments on Terra and Aqua [12]. A monthly adjustment to the SW portion of the TOT SRF as a function of wavelength ($\lambda$) is applied of the form:

$$T(\lambda) = 1 - e^{-\alpha\lambda} + \beta, \quad (3)$$

where $\alpha$ and $\beta$ are fits to the data. For each month, the appropriate correction is determined from a database of combinations of $\alpha$ and $\beta$ values. The algorithm to determine the optimal correction is based on the methodology shown in Appendix 1 of Loeb et al. [14]. Linear regression coefficients are computed for tropical mean daytime minus nighttime longwave radiances obtained using the TOT and SW channel nadir observations versus the daytime minus nighttime radiances from the WN channel nadir observations for tropical all-sky ocean and all-sky land/desert scene types with each candidate in the database. For the first month of the mission, the start of mission SRF is used to compute these regressions. For every subsequent month, the SRF from the database that results in the smallest difference in the regression fits compared to the first month of the mission is selected as the TOT channel SRF for the month. These SRFs are determined monthly for the TOT channels of each instrument independently. Starting in May 2020, the TOT channel SRFs were kept static to simplify and streamline the data production since the month-to-month SRF changes were small. However, the post-launch validation results indicated a deviation from the long-term trend starting in May 2020 (see Fig. 8). The Edition 5 version of the data products will revert to the methodology of applying monthly SRF updates.

## IV. POST-LAUNCH VALIDATION OF INSTRUMENT PERFORMANCE

The post-launch validation approach involves the use of many independent analyses at different temporal and spatial scales using various data product levels. Analyses that utilize lower-level data products generally have a stronger association with instrument performance since they involve fewer scientific algorithms. Higher-level data products provide a broader context of how instrument calibration changes impact the data products ultimately used by the scientific community. This approach provides a comprehensive end-to-end picture of instrument performance. The CERES instrument team also conducts several studies as part of a calibration-validation protocol using observations from vicarious Earth targets as well as the Moon. In this section we provide an overview of results from several analyses that demonstrate CERES instrument performance during the Terra and Aqua missions.

### *A. Tropical Mean 3-Channel Consistency Test*

The Tropical Mean 3-Channel consistency test (or TM) is a validation study used to evaluate the performance of all three channels on the CERES instrument. TM validation, which originated during the ERBE mission, involves monitoring the monthly averaged nadir viewing radiances of oceans in the tropics ($20^0$N-$20^0$S latitudes) during daytime and the nighttime. The nighttime longwave radiances are obtained directly from the TOT channel, whereas the daytime radiances are calculated using both the TOT and SW channels. In addition, a second set of daytime and nighttime longwave radiances are estimated from the WN channel by regressing the WN channel against the TOT channel during nighttime, and applying this narrowband-to-broadband conversion during daytime [15]. The trends of the differences between these two sets of daytime minus nighttime longwave radiance differences reveals any inconsistencies in the performance of the SW channel or the shortwave portion of the TOT channel. The CERES Edition 4 ERBE-like ES-8 (Level-2) data product is used for this validation experiment.

Fig. 7 shows the monthly TM day-night differences from the two methods for the FM1 instrument. The difference between the two methods (shown in green in Fig. 7) is ≈–0.5Wm$^{-2}$sr$^{-1}$, largely due to overestimation of the daytime LW from the WN channel using the narrow-to-broadband regression. Far more noteworthy is that this difference is consistent over the long-term, demonstrating the consistent performance of all three-channels over the entire period.

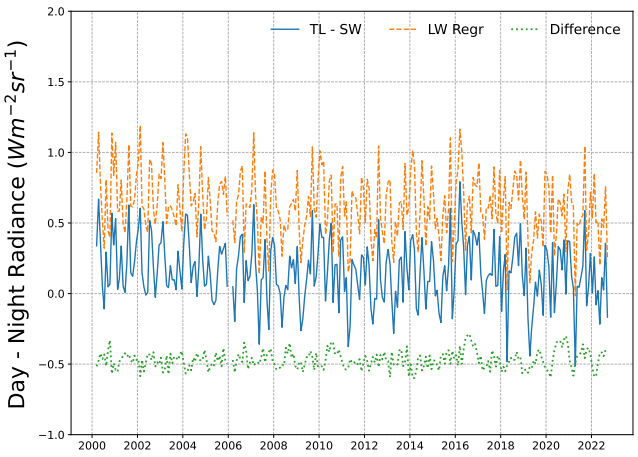


**Fig. 7.** Tropical all-sky ocean mean daytime minus nighttime LW nadir radiance difference from the TOT and SW channels (blue) and from the WN channel regression (orange) for FM1 between March 2000 and July 2022. The difference between the blue and orange lines is shown in green.

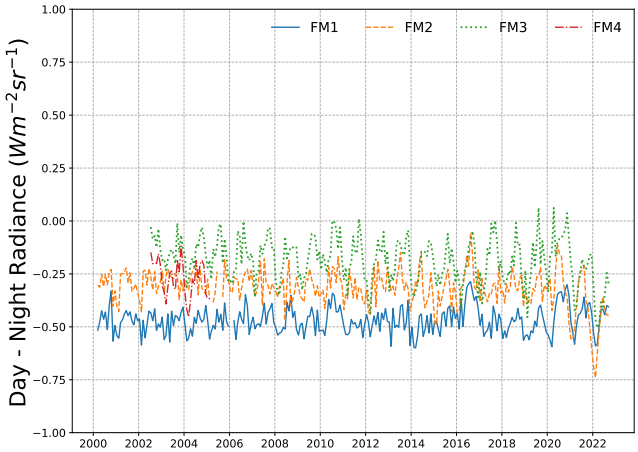


**Fig. 8.** The difference between the tropical all-sky ocean mean daytime minus nighttime longwave nadir radiance from the TOT and SW channels and estimated from the WN channel regression for CERES instruments on Terra and Aqua from the start of the missions through July 2022.

The differences between the two sets of daytime minus nighttime longwave differences for all four instruments are shown in Fig. 8. The differences are between -0.1 and -0.5 $Wm^{-2}sr^{-1}$. The relationship remains consistent for all instruments evidenced by the plots showing no discernible long-term trend. The data from Aqua/FM4 stops in March 2005, when the SW channel experienced an anomaly and did not function since then. The deviation from the long-term trend and increase in variability for FM2 and FM3 starting in June 2020 is primarily because the TOT channel SRFs are not being updated monthly. In the upcoming Edition 5 data products, these monthly SRF updates will be reinstated which will restore the consistency with the long-term trend.

*B. DCC Albedo*

Deep Convective Clouds (DCC) have many characteristics that make them ideal Earth targets for independently verifying instrument calibration. They have been used for monitoring radiometric stability of imagers [16,17,18] as well as broadband instruments like CERES [19]. Long-term trends in DCC albedo can be used to assess the stability and consistency of various CERES instruments on different platforms. To accomplish this, CERES Edition 4 SSF data products are used to identify DCC targets. A CERES footprint is identified as a DCC target if: a) it is classified as an ocean surface type, b) it is geographically located within 30°N-30°S latitude, c) its MODIS 11μm imager band brightness temperature is < 210K, d) its Viewing Zenith Angle and Solar Zenith Angle < 40 degrees, e) it has 100% cloud coverage, and f) its WN channel unfiltered radiance is < 1 $Wm^{-2}sr^{-1}$. DCC footprints are considered for this study only when the instrument is operating in the cross-track scan mode. This is especially significant during the first few years of both missions when the instruments alternated between the FAPS and RAPS modes. However, since both instruments on each spacecraft were placed into the FAPS mode in 2005 (Terra in June 2005 and Aqua in April 2005), the observations from FM1 instrument on Terra and the FM3 instrument on Aqua were used for the purposes of this analysis in 2005 and beyond.

DCC albedos are computed using data in the CERES SSF Edition 4 data product as follows:

$$A = \frac{M_{sw}}{\mu_0 E_0}, \qquad (4)$$

where $M_{sw}$ is the top-of-atmosphere (TOA) SW flux, $\mu_0=\cos(\theta_0)$, $\theta_0$ is the solar zenith angle, and $E_0$ is the observed TOA solar incoming flux (≈1361 $Wm^{-2}$) from the Total Irradiance Monitor (TIM) instrument on SORCE or TSIS.

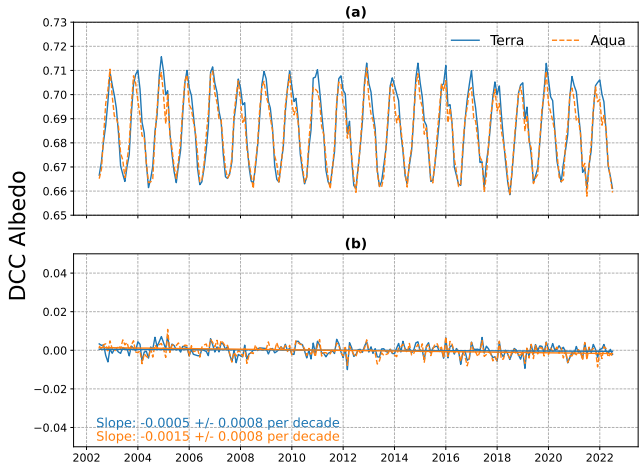


**Fig. 9.** (a) Monthly mean DCC albedos for CERES Terra and Aqua from July 2002-July 2022 and (b) corresponding DCC albedo anomalies. Also shown are the regression slopes to the anomalies and the 95% confidence intervals of the long-term trend.

Monthly mean albedos for CERES Terra and Aqua exhibit a marked seasonal cycle with both showing values ranging from

0.66 to 0.715 (Fig. 9(a)). The difference between the Terra and Aqua DCC twenty-year mean albedos is ≈0.2%. When the annual cycle is removed, monthly albedo anomalies remain within ±0.005 (Fig. 9(b)). Importantly, neither the Terra nor Aqua DCC albedo anomalies show evidence of a long-term drift. The slope of the linear regression fit to the DCC anomalies is $5\times10^{-4} \pm 8\times10^{-4}$ per decade for Terra and $1.5\times10^{-3} \pm 8\times10^{-4}$ per decade for Aqua. Even though Aqua has a small statistically significant slope, this is still extremely small.

### *C. Global Flux anomalies*

We observe the long term, global spatially and temporally averaged TOA fluxes obtained from the Level-3 CERES SSF-1deg Ed4A monthly data product for Terra and Aqua from July 2002 to July 2022. The global fluxes are broken down by surface-type: Ocean, Land or All surfaces, under all-sky conditions. The flux anomalies of the global reflected solar (SW) fluxes and Outgoing LW fluxes are computed for each spacecraft and shown in Figs. 10 and 11, respectively. Also shown in the plots are the linear regression slopes (per decade) and 95% CIs. The SSF-1deg data product only uses data from instruments operating in FAPS mode.

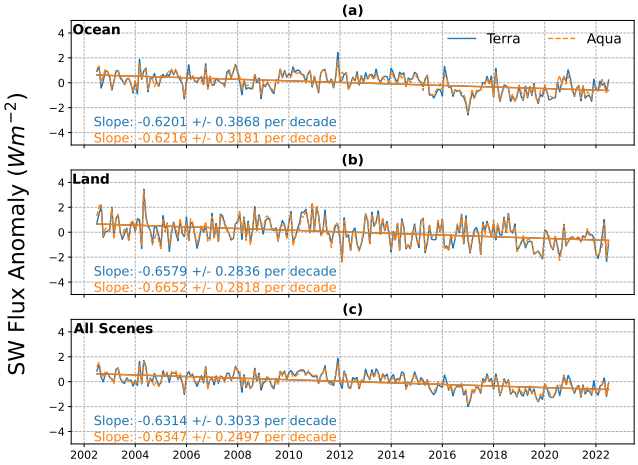


**Fig. 10.** Global SW flux anomalies for the Terra and Aqua for (a) all-sky Ocean, (b) all-sky Land and (c) all-sky all-surface footprints obtained using the CERES Edition 4 SSF-1deg data products for Jul 2002-Jul 2022. Also shown are the slopes per decade and their corresponding 95% confidence intervals.

It is seen from Fig. 10 that the SW TOA global flux anomalies for Terra and Aqua are consistent with one another and have a negative slope of 0.63±0.3 Wm$^{-2}$ per decade. The negative slope is likely due to a combination of internal climate variability and climate forcing [20]. The slopes for Terra and Aqua across all scenes are nearly identical over their common twenty-year period. The Outgoing LW flux anomalies, shown in Fig. 11, show a positive slope of ≈0.2 Wm$^{-2}$ per decade. It is clear from these plots that after incorporating all the instrument corrections, the long-term global SW and LW fluxes from the instruments on both spacecraft are remarkably consistent with each other.

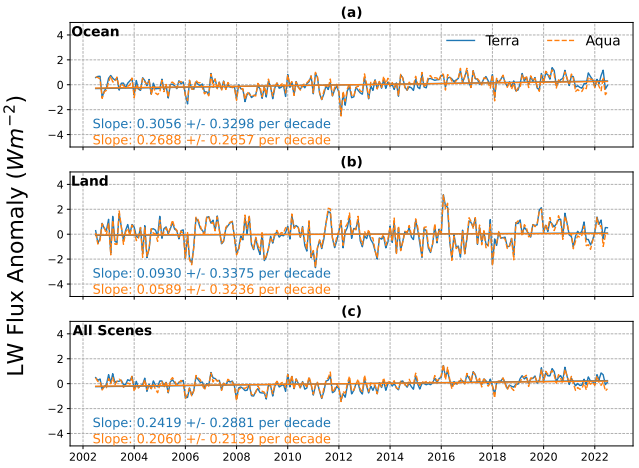


**Fig. 11.** Global Outgoing LW flux anomalies for the Terra and Aqua instruments shown for all-sky Ocean, all-sky Land and all-sky all surface footprints obtained using the CERES Edition 4 SSF-1deg data products for the twenty-year period from Jul 2002-Jul 2022. Also shown are the slopes per decade and their corresponding 95% confidence intervals.

### *D. Inter-satellite comparisons*

The nominal Terra and Aqua orbits are such that they cross one another at ≈70$^0$N at local noon and ≈70$^0$S at local midnight. This provides a unique opportunity to directly compare CERES measurements from these spacecraft while viewing the same Earth target. Given that the orbital overlaps occur at high latitudes, the comparisons are performed only during the Northern hemisphere summer months (June, July, and August), which provides sufficient reflected solar energy. During the first several years of the Terra and Aqua missions, the two instruments on each spacecraft were alternated between the FAPS and RAPS modes. To maximize the sampling, the comparisons are performed between the instruments operating in the FAPS mode. For the years 2002-2004, the comparisons were performed between the FM1 instrument and the FM4 instrument which were in the FAPS mode for most of the time during this period. However, since the SW channel on FM4 failed in March 2005, the comparisons were continued between FM1 and FM3 starting March 2005 and beyond. The criteria for establishing matched footprints are as follows: viewing zenith and solar zenith angle difference < 2 degrees, distance between footprint centroids < 7km, and relative azimuth angle difference < 5 degrees. All Aqua-Terra differences for the matched footprints obtained during the three months considered in a year are averaged to a single value for the year. For the SW measurements, the differences are computed using monthly reflectance (R) derived from the SW unfiltered radiances as follows:

$$R = \frac{SWrad * \pi}{F * \cos(SZA)}, \tag{5}$$

where *SWrad* is the SW unfiltered radiance, *F* is the solar insolation at the top of the atmosphere (1361 W/m$^2$), and *SZA* is the solar zenith angle of the footprint under consideration.

The computations are performed using the CERES SSF Edition-4 data products.

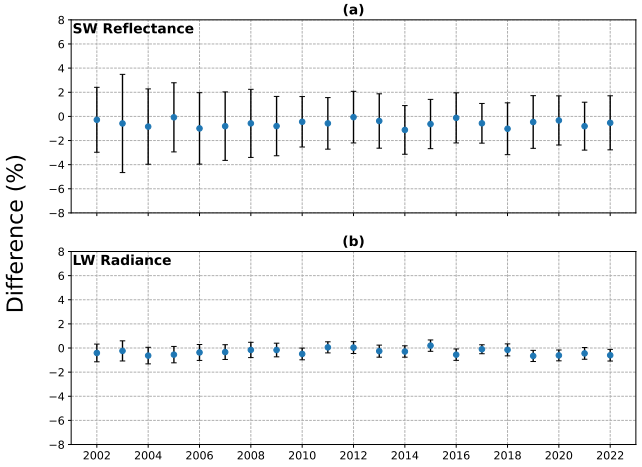


**Fig. 12.** CERES Aqua-Terra differences of (a) SW Reflectance and (b) Daytime LW radiance during Aqua and Terra orbital crossings.

For the daytime LW, the differences are computed on the radiances. The daytime longwave radiances are obtained using the TOT and SW channels. Fig. 12(a) and (b) show the monthly comparisons between Aqua-Terra for the SW reflectance and daytime LW radiance, respectively, along with their associated 95% CI. The differences of SW reflectance and the daytime LW radiances demonstrate slight annual variability associated with the seasonal cycles. In addition, there are no statistically significant differences between Terra and Aqua over the twenty-year period for the SW reflectance and the daytime LW radiance, indicating consistency between the instruments on both spacecraft.

*E. Lunar Observations*

CERES instruments on Terra and Aqua have been viewing the Moon consistently since 2006. The Moon is an inadequate source to calibrate the CERES instruments at the level of accuracy desired. The Moon underfills the CERES instrument FOV, which presents challenges for absolute calibration. The uncertainties in the Moon's spectral knowledge and viewing geometries far exceed the measurement uncertainty of CERES. However, once the CERES lunar observations are appropriately corrected for its non-ideal characteristics, they can be useful for verifying the telescope's pointing knowledge, co-alignment between the three telescopes on an instrument, spatial uniformity of the dynamic response of the sensor channels and to instrument performance [21].

Lunar views from CERES are obtained 5 orbits prior and 5 orbits after each full Moon. The lunar observations with CERES involve fixing the scanner's elevation position and rotating in azimuth as the Moon passes through the plane of the FOV. The resulting non-uniform zig-zig data pattern with respect to instrument FOV are translated into a standard grid of FOV azimuth and elevation position using Delaunay triangulation. The data obtained from lunar views are then corrected for the sensor's point response, Earth-Sun distance, Earth-Moon distance, lunar phase angles and lunar libration.

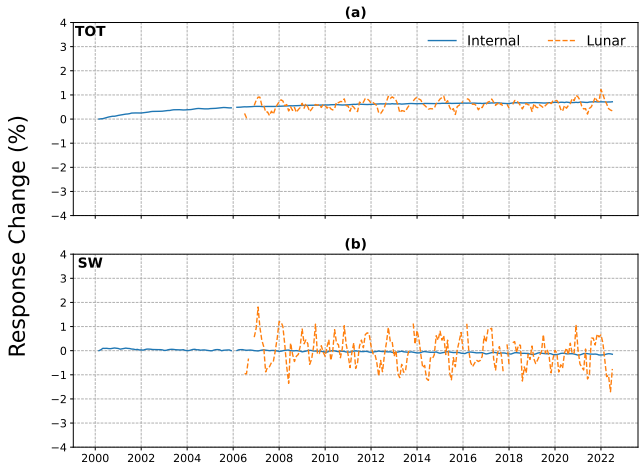


**Fig. 13.** Long-term trend of Lunar observations, normalized to the first month of observations, from the TOT and SW channels overlayed on the gains (from the ICM) of the corresponding channels for the instruments on FM1.

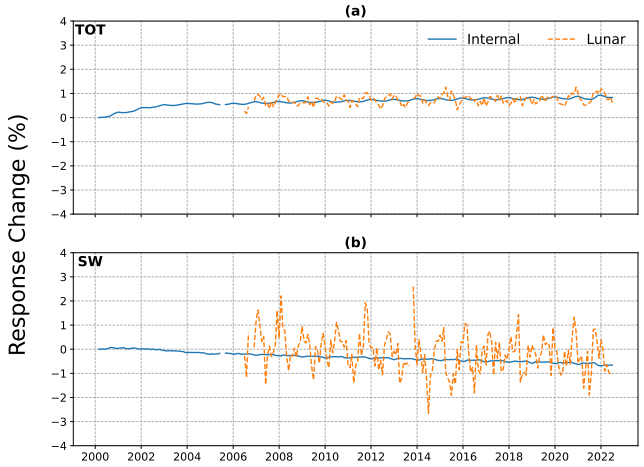


**Fig. 14.** Long-term trend of Lunar observations, normalized to the first month of observations, from the TOT and SW channels overlayed on the gains (from the ICM) of the corresponding channels for the instruments on FM2.

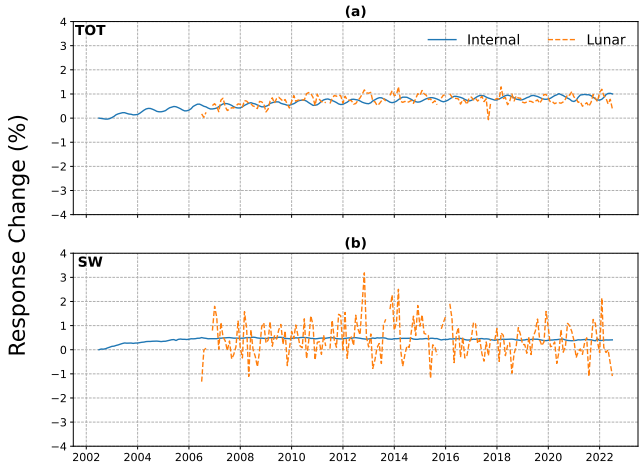


**Fig. 15.** Long-term trend of Lunar observations, normalized to the first month of observations, from the TOT and SW channels

overlayed on the gains (from the ICM) of the corresponding channels for the instruments on FM3.

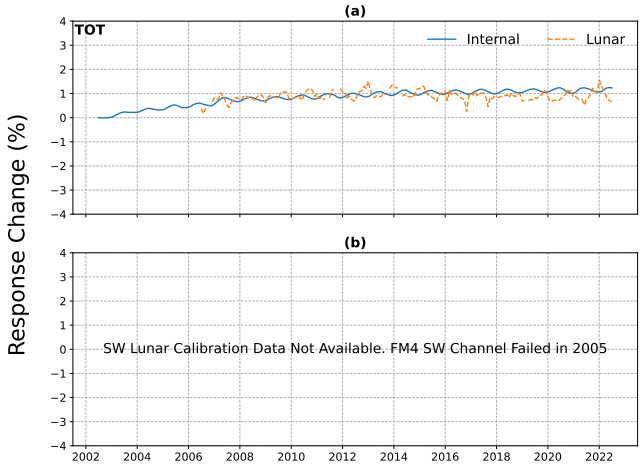


**Fig. 16.** Long-term trend of lunar observations, normalized to the first month of observations, from the TOT and SW channels overlayed on the gains (from the ICM) of the corresponding channels for the instruments on FM4.

The monthly lunar observations from the SW and TOT channels from each instrument are the digital counts normalized to the first available month of data after all the corrections have been applied. Since the channel digital counts are used for the trending, the effects of change of gain or SRF with time are not accounted for in this analysis. Figs. 13-16 show the long-term trends of lunar observations from the instruments on Terra and Aqua for the period March 2006- July 2022. Any gaps in the plots are due to missing lunar observations for the month. Also shown are the Edition 4 gains for the corresponding channels overlayed on the lunar data. For FM4, the SW channel failed in March 2005, and therefore, no lunar observations are available.

It is observed that the lunar observations from CERES have large month-to-month variability even after applying all known corrections to the observations to account for viewing geometry and lunar libration. This variability is significantly larger for the SW channel than the TOT channel because of the lower signal levels in the SW. Furthermore, the variability far exceeds that of the monthly gains from the ICM. It is also seen that the long-term trends from the lunar observations generally follow those from the internal calibration. The results indicate that after the known corrections are applied to the CERES lunar observations, they can track the long-term large changes to the instrument response. However, the month-to-month variability of these observations is too large for the Moon to be used to calibrate CERES. In addition, consistent views of the Moon from CERES on Terra and Aqua started only in 2006, which is several years after the largest changes in SW and TOT channel gains were observed at the start of their respective missions. Therefore, the CERES team does not use the Moon for calibrating CERES instruments. There is ongoing work to build and launch instruments to make important advances in characterizing the Moon for calibrating space-based imagers and radiometers [22, 23]. The CERES team will incorporate any additional corrections to the CERES data based on knowledge gained from these missions.

## CONCLUSIONS

The CERES instruments on the Terra and Aqua missions have provided a continuous global record of the TOA fluxes for over twenty years, well beyond the instruments' design lifetime of five years. To ensure that CERES instruments provide data with consistent quality, each instrument underwent a rigorous pre-launch calibration and characterization campaign, which involved calibrating the on-board calibration sources to a common traceable radiometric reference. Once in flight, the CERES team monitors each channel's broadband performance (gains) through the on-board calibration sources. Given the unique set of measurements CERES provides, no single calibration source (or vicarious target) can provide all the data necessary to calibrate or validate the instrument. As a result, the CERES team performs a suite of validation experiments using Earth targets as well as the Moon, spanning a range of spatial, temporal and spectral scales with each experiment to provide a comprehensive assessment of instrument performance.

The CERES team periodically updates the calibration and validation protocol based upon lessons learned from analyzing the data over many years. These updates are incorporated into the latest releases of the CERES data products. The current version of the CERES Terra and Aqua data products is Edition 4. The CERES team continues to revisit the existing calibration/validation algorithms and will update these as necessary in the upcoming Edition 5 data products.

In this paper, we demonstrate that after applying calibration adjustments (i.e., broadband radiometric gain and the time varying SRFs) for the SW and TOT channels, the CERES instruments on Terra and Aqua are extremely stable and consistent with one another. Terra-Aqua inter-comparisons are also evaluated during spacecraft orbital crossovers and these show no statistically significant differences or long-term trends, further confirming the consistency between the instruments. The lunar observations, started in 2006, show large variability and therefore cannot be used as a stand-alone calibration target for CERES. However, their long-term trends mimic those from on-board calibration sources, providing an added validation tool.

## REFERENCES

[1] N. G. Loeb, D. R. Doelling, H. Wang, W. Su, C. Nguyen, J. G. Corbett, L. Liang, C. Mitrescu, F. G. Rose, and S. Kato, "Clouds and the Earth's Radiant Energy System (CERES) Energy Balanced and Filled (EBAF) Top-of-Atmosphere (TOA) Edition 4.0 Data Product", J. Climate, 31(2), 895–918, 2018, https://doi.org/10.1175/JCLI-D-17-0208.1

[2] B. A. Wielicki, B. R. Barkstrom, E.F. Harrison, R. B. Lee III, G. L. Smith, and J. E. Cooper, "Cloud's and the Earth's Radiant Energy System (CERES): An Earth Observing System Experiment," Bull. Amer. Meteor. Soc. 77, 853–868 (1996), https://doi.org/10.1175/1520-0477(1996)077<0853:CATERE>2.0.CO;2

[3] R. S. Wilson, K. J. Priestley, S. Thomas, and P. Hess "On-orbit solar calibration methods using the Clouds and Earth's Radiant Energy System (CERES) in-flight calibration system", Proc. SPIE 8510, Earth Observing Systems XVII, 851003 (15 October 2012), https://doi.org/10.1117/12.930922

[4] W. Su, J. Corbett, Z. Eitzen, and L. Liang, "Next-generation angular distribution models for top-of-atmosphere radiative flux calculation from

CERES instruments: methodology", Atmos. Meas. Tech., 8, 611–632, 2015, https://doi.org/10.5194/amt-8-611-2015

[5] R. B. Lee III, B. R. Barkstrom, H. C. Bitting, D. H. Crommelynck, J. Paden, D. K. Pandey, K. J. Priestley, G.L. Smith, S. Thomas, K. L. Thornhill, R. S. Wilson, "Prelaunch calibrations of the Clouds and the Earth's Radiant Energy System (CERES) Tropical Rainfall Measuring Mission and Earth Observing System Morning (EOS-AM1) spacecraft thermistor bolometer sensors", IEEE Transactions on Geoscience and Remote Sensing, Vol 36, No. 4, 1173 - 1185, July 1998, https://doi.org/10.1109/36.701024

[6] K. J. Priestley, B. R. Barkstrom, R. B. Lee III, R. N. Green, S. Thomas, R. S. Wilson, P. L. Spence, J. Paden, D. K. Pandey, A. Al-Hajjah, "Postlaunch Radiometric Validation of the Clouds and the Earth's Radiant Energy System (CERES) Proto-Flight Model on the Tropical Rainfall Measuring Mission (TRMM) Spacecraft through 1999", Journal of Applied Meteorology, 39(12), 2249-2258. https://doi.org/10.1175/1520-0450(2001)040<2249:PRVOTC>2.0.CO;2

[7] N. G. Loeb, K. J. Priestley, D. P. Kratz, E. B. Geier, R. N. Green, B. A. Wielicki, P. O. Hinton, and S. K. Nolan, "Determination of Unfiltered Radiances from the Clouds and the Earth's Radiant Energy System Instrument", Journal of Applied Meteorology (1988-2005), 40(4), 822–835, https://doi.org/10.1175/1520 0450(2001)040<0822:DOURFT>2.0.CO;2

[8] Z. P. Szewczyk, K. J. Priestley, D. R. Walikainen, N. G. Loeb, G. L. Smith, "Putting all CERES instruments (Terra/Aqua) on the same radiometric scale," Proc. SPIE 8177, Remote Sensing of Clouds and the Atmosphere XVI, 817704 (26 October 2011); https://doi.org/10.1117/12.896897

[9] R.S. Wilson, K. J. Priestley, S. Thomas, P. Hess "On-orbit solar calibrations using the Clouds and the Earth's Radiant Energy System (CERES) in-flight calibration system," Optical Sci., Eng. & Instrum., Proc.SPIE vol. 4135-03, August 2009, https://doi.org/10.1117/12.862172

[10] R. S. Wilson, K. J. Priestley, S. Thomas, P. Hess, M. Shankar, N. Smith, and P. Szewczyk "On-orbit solar calibration methods using the Clouds and Earth's Radiant Energy System (CERES) in-flight calibration system: lessons learned", Proc. SPIE 8866, Earth Observing Systems XVIII, 886607 (23 September 2013); https://doi.org/10.1117/12.2025967

[11] S. Thomas, K. J. Priestley, N. M. Smith, N. G. Loeb, P. C. Hess, M. Shankar, D. R. Walikainen, Z. P. Szewczyk, R. S. Wilson, D. L. Cooper, "Characterization of the clouds and the Earth's radiant energy system (CERES) sensors on Terra and Aqua spacecraft," Proc. SPIE 7862, Earth Observing Missions and Sensors: Development, Implementation, and Characterization, 78620N (11 November 2010); https://doi.org/10.1117/12.869684

[12] N. G. Loeb, N. Manalo-Smith, W. Su, M. Shankar, and S. Thomas, "CERES Top-of-Atmosphere Earth Radiation Budget Climate Data Record: Accounting for in-Orbit Changes in Instrument Calibration", Remote Sensing, 8, no. 3: 182, 2016, https://doi.org/10.3390/rs8030182

[13] L. G. Clark, J. D. Dibattista, "Space qualification of optical instruments using NASA long duration exposure facility", Opt. Eng. 1978, 17, 547–552, https://doi.org/10.1117/12.7972276

[14] N. G. Loeb, S. Kato, W. Su, T. Wong, F. G. Rose, D. R. Doelling, J.R. Norris, and X. Huang, "Advances in understanding top-of-atmosphere radiation variability from satellite observations", Springer, Surv. Geophys., 33, 359-385, 2012, https://doi.org/10.1007/s10712-012-9175-1

[15] G. L. Smith, S. Thomas, K. J. Priestley, and D. R. Walikainen, "Tropical Mean Fluxes: A Tool for Calibration and Validation of CERES Radiometers," in *IEEE Transactions on Geoscience and Remote Sensing*, vol. 54, no. 9, pp. 5135-5142, Sept. 2016, https://doi.org/ 10.1109/TGRS.2016.2556581

[16] D. R. Doelling, D. Morstad, B. R. Scarino, R. Bhatt and A. Gopalan, "The Characterization of Deep Convective Clouds as an Invariant Calibration Target and as a Visible Calibration Technique," in *IEEE Transactions on Geoscience and Remote Sensing*, vol. 51, no. 3, pp. 1147-1159, March 2013, https://doi.org/10.1109/TGRS.2012.2225066

[17] R. Bhatt, D. R. Doelling, B. Scarino, C. Haney, A. Gopalan, "Development of Seasonal BRDF Models to Extend the Use of Deep Convective Clouds as Invariant Targets for Satellite SWIR-Band Calibration", *Remote Sens.* 2017, *9*, 1061, https://doi.org/10.3390/rs9101061.

[18] Y. Hu, B. A. Wielicki, P. Yang, P. W. Stackhouse, B. Lin and D. F. Young, "Application of deep convective cloud albedo observation to satellite-based study of the terrestrial atmosphere: monitoring the stability of spaceborne measurements and assessing absorption anomaly," in *IEEE Transactions on Geoscience and Remote Sensing*, vol. 42, no. 11, pp. 2594-2599, Nov. 2004, https://doi.org/10.1109/TGRS.2004.834765

[19] D. P. Kratz, K. J. Priestley, and R. N. Green, "Establishing the relationship between the CERES window and total channel measured radiances for conditions involving deep convective clouds at night", J. Geophys. Res., 107( D15), 2002, https://doi.org/10.1029/2001JD001170

[20] N. G. Loeb, T. J. Thorsen, J. R. Norris, H. Wang, W. Su, "Changes in earth's energy budget during and after the "pause" in global warming: An observational perspective", Climate 2018, 6, 62, https://doi.org/10.3390/cli6030062

[21] J. L. Daniels, G. L. Smith, K. J. Priestley, and S. Thomas, "Using Lunar Observations to Validate In-Flight Calibrations of Clouds and the Earth's Radiant Energy System Instruments," in *IEEE Transactions on Geoscience and Remote Sensing*, vol. 53, no. 9, pp. 5110-5116, Sept. 2015, https://doi.org/10.1109/TGRS.2015.2417314

[22] R. Swanson, M. Kehow, M. Stebbins, H. Courrier, T. Jackson, C. Lukashin, M. Cooney, W. Davis, G. Kopp, P. Smith, C. Buleri, T. Stone, "The ARCSTONE Project to Calibrate Lunar Reflectance," 2020 IEEE Aerospace Conference, Big Sky, MT, USA, 2020, pp. 1 – 10, https://doi.org/10.1109/AERO47225.2020.9172629

[23] B. A. Wielicki, et al.. (2013). Achieving Climate Change Absolute Accuracy in Orbit. Bulletin of the American Meteorological Society 94, 10, 1519-1539, https://doi.org/10.1175/BAMS-D-12-00149.1